Spatiotemporal Changes in Diffusivity and Anisotropy in Fetal Brain Tractography

Fedel Machado-Rivas
Department of Radiology, Boston Children's Hospital
Onur Afacan
Department of Radiology, Boston Children's Hospital
Shadab Khan
Department of Radiology, Boston Children's Hospital
Bahram Marami
Department of Radiology, Boston Children's Hospital
Clemente Velasco-Annis
Department of Radiology, Boston Children's Hospital
Hart Lidov
Department of Pathology, Boston Children's Hospital
Simon Warfield
Department of Radiology, Boston Children's Hospital
Ali Gholipour
Department of Radiology, Boston Children's Hospital
Camilo Jaimes (camilo.jaimescobos@childrens.harvard.edu)
Department of Radiology, Boston Children's Hospital

Research Article

Keywords: Fetal, Tractography, Atlas, Diffusion, Anisotropy, Myelination

DOI: https://doi.org/10.21203/rs.3.rs-150845/v1

Abstract

Population averaged diffusion atlases can be utilized to characterize complex microstructural changes with less bias than data from individual subjects. In this study, a fetal diffusion tensor imaging (DTI) atlas was used to investigate tract-based changes in anisotropy and diffusivity in vivo from 23 to 38 weeks of gestational age (GA). Healthy pregnant volunteers with typically developing fetuses were imaged at 3 Tesla. Acquisition included structural images processed with a super-resolution algorithm and DTI images processed with a motion-tracked slice-to-volume registration algorithm. The DTI from individual subjects were used to generate 16 templates, each specific to a week of GA; this was accomplished by means of a tensor-to-tensor diffeomorphic deformable registration method integrated with kernel regression in age. Deterministic tractography was performed to outline the forceps major, forceps minor, bilateral corticospinal tracts (CST), bilateral inferior fronto-occipital fasciculus (IFOF), bilateral inferior longitudinal fasciculus (ILF), and bilateral uncinate fasciculus (UF). The mean fractional anisotropy (FA) and mean diffusivity (MD) was recorded for all tracts. For a subset of tracts (forceps major, CST and IFOF) we manually divided the tractograms into anatomy conforming segments to evaluate within-tract changes. We found tract-specific, non-linear, age related changes in FA and MD. Early in gestation, these trends appear to be dominated by cytoarchitectonic changes in the transient white matter fetal zones while later in gestation, trends conforming to the progression of myelination were observed. We also observed significant (local) heterogeneity in within-tract developmental trajectories for the CST, IFOF, and forceps major.

Introduction

Development of the fetal brain in the second and third trimesters is remarkably complex. In addition to rapid growth, a series of cellular changes take place, including neuronal proliferation and migration, axonal growth and pruning, dendritic sprouting, synapse formation, and myelination[1–3]. These processes are frequently analyzed in the context of findings on structural *in vivo* and *ex vivo* fetal MRI and include the progressive decrease in volume of the proliferative compartment (ventricular and subventricular zone) after the 25th week of gestational age (GA), the growth and subsequent involution of several transient compartments (intermediate zone and subplate), and the expansion and folding of the cortical plate[4 5]. While these volumetric analyses provide valuable insights into brain growth, they are insensitive to many cellular events that occur during this critical period in development.

Diffusion tensor imaging (DTI) offers complementary information to structural imaging by probing tissue characteristics such as cellularity, water content, and tissue coherence. Due to the challenges related to subject motion, the early studies on fetal DTI consisted of *ex vivo* analysis. Huang et al[6], showed that diffusion imaging could demonstrate the various layers of the cerebral wall in fetuses between 13 and 21 weeks of GA and that tractography of major white matter bundles was possible even at this early GA. Song et al[7], utilized ex-vivo tractography to characterize the developmental trajectories in major white matter pathways in fetuses, newborns, and infants; the focus of this study was on whole-tract maturation

along a broad lifespan (> 3 years) and did not consider local factors influencing these changes in fetal life. The study by Xu et al[8] documented that the radial glial fibers are the main determinant of anisotropy in the white matter of second trimester fetuses, thereby linking the process of neuronal migration and the regression of this glial scaffolding to changes in DTI parameters. A major leap in microstructural analysis of brain maturation was the development of motion correction algorithms for *in vivo* fetal DTI. Even though *in vivo* analysis of fetal brain microstructure with DTI and DTI-based tractography had been described previously by Schneider et al[9], Kasprian et al[10], and others, the advent of these motion correction algorithms enabled robust quantitative analysis *in vivo*. Importantly, most of the data available on tract-specific maturational changes is limited to third trimester fetuses, at a time where myelination drives the changes in diffusivity[11]; this data is also limited to whole-tract (tract-average) metrics. The physiologic changes in the transient fetal compartments that occur in the second and early third trimester and how these shape local diffusivity properties of the traversing white matter tracts remains unexplored.

Population averaged diffusion atlases can be utilized to characterize complex microstructural changes with less bias than data from individual subjects[12]. This is particularly important when characterizing data sets with relatively low SNR, such as fetal DTI. The first reported application of atlas-based techniques to characterize microstructural fetal brain development were based on *ex vivo* data[13]. The introduction of motion corrected fetal DTI in individual subjects enabled Khan and colleagues to create the first atlas of fetal DTI using *in vivo* data; this atlas depicts microstructural changes in high anatomic detail across a broad prenatal age range[14]. The purpose of this study is to utilize atlases of fetal brain DTI built from in vivo subjects to investigate tract-based changes with high spatiotemporal resolution. We hypothesized that the atlas-based tractography would be able to individually demonstrate the effects of the involution of the transient fetal zones and the subsequent onset of myelination. Furthermore, we expected to be able to characterize local (within-tract) developmental trajectories driving tract-averaged microstructural changes.

Materials And Methods

Study Population

This was a HIPAA compliant study approved by the Institutional Review Board of Boston Children's Hospital, all methods were performed in accordance with the relevant guidelines and regulations. Participants were prospectively recruited and informed consent was obtained prior to the MRI. Criteria for inclusion were: a) normal pregnancy between 20 and 40 weeks of gestational age (GA), b) maternal age between 18 and 45 years, and c) lack of significant prior medical history in the mother. Exclusion criteria were: (a) maternal contraindication to MRI, (b) suspected or confirmed congenital infection in the fetus, (c) brain or other organ abnormalities in the fetus (known or identified on the fetal MRI), (d) chromosomal aberrations, and (e) multiple-gestation pregnancy.

Image Acquisition:

Subjects were imaged on 3 Tesla (T) MRI scanners (Skyra or Prisma, Siemens Medical Solutions, Erlangen, Germany) using spine and 18-channel body coils. The structural imaging protocol consistent of multiple T2-weighted Half-Fourier-Acquired Single-shot Turbo spin Echo (HASTE) scans in orthogonal planes, with the following acquisition parameters: time to repetition (TR) = 1400–2000ms, Time to echo (TE) = 100–120 ms, 2 or 4 slice interleaved acquisitions, 0.9–1.1 mm in-plane resolution, 2–3 mm slice thickness without gap, matrix size = 256x204, 256x256, or 320x320 with. The DTI protocol consisted of three to eight scans, also along orthogonal planes with respect to the fetal head. In each scan, 1 or 2 b = 0 s/mm2 images, and 12 diffusion-sensitized images at b = 500 s/mm2 were acquired. Acquisition parameters were: TR = 3,000–4,000 ms, TE = 60 ms, in-plane resolution = 2 mm, slice thickness = 2–4 mm.

Image processing:

Structural images for individual subjects were processed according to a previously validated slice-to-volume reconstruction (SVR) algorithm that uses 2D low-resolution HASTE images to generate 3D super resolution and intensity normalized volumetric image of the fetal brain [15]. The fetal DTI data was processed as described by Marami et al[16], with a robust motion-tracked (MT)-SVR approach; this reconstruction method discards motion corrupted diffusion sensitized images, registers the non-corrupted data to a common space, and leverages the redundancy obtained through serial/repeated acquisitions to allow for a robust estimation of the diffusion tensor, despite partial rejection of data[17].

DTI Atlas Construction

A spatiotemporal atlas of fetal brain DTI was created using the data from individual subjects. The framework utilized was described by Khan et al[14], and consists of a tensor-to-tensor diffeomorphic deformable registration integrated with kernel regression in age[14]. To build the atlas, we utilized images from 67 high quality examinations with optimal MT-SVR diffusion reconstructions, devoid of obvious artifacts; these were used to generate 16 templates, each corresponding to a specific week of GA. The number and sex of subjects included for each gestational week template is described in Table 1.

Tractography Processing and Tract Segmentation

Each individual gestational week diffusion tensor template was processed using Diffusion Toolkit (Version 0.6.4.1, Athinoula A. Martinos Center for Biomedical Imaging, Massachusetts General Hospital, Boston, MA)[18] with a deterministic fiber assignment by a continuous tracking (FACT) algorithm. A 35° angle threshold and automatic FA thresholding were used to perform tractography by user-defined regions of interest (ROI)[18]. A research fellow with medical training drew inclusion and exclusion ROIs TrackVis (Trackvis 0.6.1 Athinoula A. Martinos Center for Biomedical Imaging, Massachusetts General Hospital)[18] to delineate the forceps major, forceps minor, bilateral corticospinal tracts (CST), bilateral inferior fronto-occipital fasciculus (IFOF), bilateral inferior longitudinal fasciculus (ILF), and bilateral uncinate fasciculus (UF) as previously described by Macedo Rodrigues et al[19] and Catani et al[20]. This set of adjusted labels was shown to result in high-quality fetal tractography by Jaimes et al[11].

We performed whole-tract analysis by extracting the mean FA and ADC for each individual week template and tract. To evaluate local variation in diffusion metrics we performed a sub analysis of three tracts: the CST, forceps major, and IFOF. These tracts were selected because they represent projection, commissural, and association fibers respectively, and have been reported to change rapidly with GA prenatally[11]. These tracts were segmented into various components using ITK-SNAP[21]. The CST was divided in an inferior segment extending from the medulla inferiorly to the midbrain superiorly (terminating at the level of the red nucleus and cerebral peduncle), a mid-segment extending from the lower aspect of the internal capsule to the inferior edge of the corpus callosum, and a superior segment extending from the corpus callosum to the cerebral cortex. The IFOF was subdivided into an anterior segment extending from the frontal cortex to the genu of the internal capsule, a mid-segment extending from the genu of the internal capsule to the periatrial white matter at the level of the splenium of the corpus callosum, and a posterior segment extending from here to the occipital cortex. The forceps major was divided into a central segment and two (right/left) hemispheric segments that extended from the temporo-occipital fissure to the cortex. The output of the ROI based tractography and the segmental tract analysis was reviewed and revised as needed by a board certified pediatric neuroradiologist with experience in fetal neuroimaging.

Statistical Analysis

A linear regression analysis was used to evaluate gestational age as predictor of FA and MD. Laterality (left or right) was included as a covariate for CST, IFOF, ILF, and UF. Linear splines with a pre-specified knot at 30 gestational weeks ($\leq$ 30 weeks, > 30 weeks) were introduced to the model if deemed appropriate by visual inspection of scatterplots and overall fit of the model as measured by adjusted R^2. This time-point was preliminarily chosen as it represents the time at which the transient fetal white matter zones start to involute. Level of significance was set at an α value of 0.05 for all tests. Stata 15/ EC (StataCorp, College Station, TX, USA) was used for all tests and graphs.

Results

All white matter tracts were successfully delineated in the GA-specific diffusion templates. Figure 1 illustrates robust outcome of tractography across the GAs studied.

Whole-tract Analysis:

Commissural Tracts

Forceps major and forceps minor tracts were delineated for all gestational ages (Table 2); there was no premature termination of tractography, with both ends of each tract extending to the cortex. In the forceps major, FA significantly increased across all GAs studied ($P < 0.001$). In the forceps minor, FA significantly decreased with GA at < 30 weeks, while in GA $\leq$ 30 weeks FA change was not significant ($P = 0.532$) (Fig. 2a, 2b).

In the forceps major MD increased significantly with GA at ≤ 30 weeks (P = 0.014) and significantly decreased with GA at > 30 weeks (P < 0.001). In the forceps minor, MD also increased significantly with GA at ≤ 30 weeks (P < 0.001), and significantly decreased with GA at > 30 weeks (P = 0.006) (Fig. 2c, 2d).

Projection Tracts

Left and right CST were delineated for all gestational ages (Table 2). In templates for low GA (< 27 weeks), the tracts did not reach the cortical plate and the tractography terminated the intermediate zone, before reaching the subplate. In templates for the rest of GAs, tractography reached the cortical plate. At < 30 weeks there was no significant change in FA with increasing GA (P = 0.620). FA significantly increased with GA at > 30 weeks (P < 0.001). There was no significant difference in FA (P = 0.886) between right and left tracts accounting for GA (Fig. 3a).

MD significantly increased with GA at ≤ 30 weeks (P = 0.001), and significantly decreased with GA > 30 weeks (P < 0.001). Similarly, there was no significant difference in MD (P = 0.960) between right and left tracts accounting for GA (Fig. 3b).

Association Tracts

Left and right IFOF, ILF, and UF were delineated for all gestational ages (Table 2). In the IFOF, FA significantly decreased with GA at ≤ 30 weeks (P = 0.002), and significantly increased with GA at > 30 weeks (P < 0.001). There was no significant difference in FA between right and left IFOF accounting for GA (P = 0.062). In the ILF, FA significantly decreased with GA at ≤ 30 weeks (P < 0.001), and significantly increased with GA at > 30 weeks (P < 0.001). There was no significant difference in FA between right and left ILF accounting for GA (P = 0.189). In the UF, FA was not significantly associated with GA at ≤ 30 weeks (P = 0.717), but significantly increased with GA at > 30 weeks (P < 0.001). As before, there was no significant difference in FA between right and left UF accounting for GA (P = 0.990) (Fig. 4a, 4b, 4c).

MD significantly increased in the IFOF with GA at ≤ 30 weeks (P < 0.001), and significantly decreased with GA at > 30 weeks (P < 0.001). There was no significant difference in MD between right and left IFOF accounting for GA (P = 0.081). For the ILF, MD significantly increased with GA at ≤ 30 weeks (P < 0.001), and significantly decreased with GA at > 30 (P < 0.001). Similarly, there was no significant difference in MD between right and left ILF accounting for GA (P = 0.887). For the UF, MD significantly increased with GA at > 30 weeks (P = 0.011), and significantly decreased with GA at ≤ 30 weeks (P < 0.001). Again, there was no significant difference in MD between right and left ILF accounting for GA (P = 0.845) (Fig. 4d, 4e, 4f).

Local changes (within-tract analysis):

Commissural Tracts

Forceps major segments (central and peripheral) were analyzed for all GA (Table 3). FA increase in the central segment was not statistically significant (P = 0.106). In the peripheral segments, FA significantly

increased with GA at ≤ 30 weeks (P < 0.001), but was not significantly associated with GA at > 30 weeks (P = 0.877).

MD for the central segment did not change significantly with GA at < 30 weeks (P = 0.215), while it significantly decreased with GA > 30 weeks (P < 0.001). For the peripheral segment, MD significantly increased with GA ≤ 30 weeks (P = 0.002), and significantly decreased with GA at > 30 weeks (P < 0.001) (Fig. 5).

Projection Tracts

CST segments (superior, middle, and inferior) were analyzed for all GA (Table 3). FA in the superior segment significantly decreased with GA 30 at ≤ weeks (P < 0.001), and significantly increased with GA at > 30 weeks (P < 0.001). In the middle segment, FA significantly increased with all GA (P < 0.001). In the inferior segment, FA significantly increased with GA at ≤ 30 (P = 0.009), but was not significantly associated with GA at > 30 weeks (P = 0.494).

In the superior segment MD significantly decreased GA across the entire data set (P = 0.006). Similarly, MD in the middle segment significantly decreased with GA for all templates (P = 0.020). In the inferior segment, MD was not significantly associated with GA (P = 0.298) (Fig. 6).

Association Tracts

Results for the individual segments (rostral, middle, and caudal) of the IFOF are summarized in Table 3. FA in the anterior segment significantly decreased with GA ≤ 30 weeks (P < 0.001), but was not significantly associated with GA at > 30 weeks (P = 0.631). In the middle segment, FA was not significantly associated with GA at ≤ 30 weeks (P = 0.680), but significantly increased with GA at > 30 weeks (P = 0.001). In the posterior segment, FA significantly decreased with GA at ≤ 30 (P < 0.001), and significantly increased with GA at > 30 weeks (P = 0.006).

Comparatively, the MD in the anterior segment significantly increased with GA at ≤ 30 weeks (P < 0.001), and significantly decreased with GA at > 30 weeks (P = 0.008). Similarly, in the middle segment MD significantly increased with GA at ≤ 30 weeks (P = 0.010), and significantly decreased with GA at > 30 weeks (P = 0.001). In the posterior segment, MD also significantly increased with GA ≤ 30 weeks (P < 0.001), and significantly decreased with GA > 30 weeks (P < 0.001) (Fig. 7).

Discussion

The advent of motion robust fetal DTI permitted in vivo characterization of brain microstructural development[11]. The construction of spatiotemporal atlases of fetal brain DTI have further enabled analysis of many developmental changes at early GAs despite the small size of the structures and the relatively low SNR of the individual acquisitions. In this study we utilized an atlas-based approach to evaluate tract-specific microstructural changes and their relationship to other important cytoarchitectonic processes. Our atlas-based diffusion tractography shows a series of tract-specific, age-related changes in

FA and MD. While the changes in the later part of gestation (> 30 weeks) conform to expected post-natal trajectories depicting an increase in FA and a decrease in MD, these trends are unapparent or appear reversed in several major white matter tracts earlier in gestation (22–29 weeks). This divergence indicates that at earlier developmental stages different biologic processes drive diffusivity and anisotropy in the parenchyma and consequently along the traversing white matter tracts. In addition, our segment-based analysis of selected commissural, projection, and association tracts demonstrates considerable within-tract heterogeneity in maturation, with distinct local developmental trajectories.

Two anatomically overlapping yet biologically distinct and asynchronous processes take place in the brain in the second half of gestation: (a) the evolution of the transient zones of the fetal telencephalon and (b) the onset and progression of myelination. Early in the second trimester, the telencephalon is organized in concentric layers, most of which are visible on MRI. The outermost layer or cortical plate (CP) contains post-migratory neurons and shows high FA and low MD early in gestation; as the CP matures, dendritic arborization and synapse formation mediate an increase in intercellular space that leads to loss of FA and higher diffusivity[22]. Beneath the CP, there is a water rich and relatively acellular layer characterized by high MD and very low FA, known as the subplate (SP)[8,23]. The SP increases in thickness and volume during the second and early third trimester, with a reported peak at approximately 30 weeks of GA when it occupies up to 45% of the volume of the telencephalon [6]. The intermediate zone (IZ) is the deep layer subjacent to the SP, which contains migrating neurons and organized axonal bundles that result in moderately low MD and high FA. Overtime, the progressive loss of the radial glial scaffolding and the dispersion of the migrating neurons results in a loss of FA and increase in MD[8,23]. After 30 weeks of GA, the subplate and intermediate zone undergo reorganization and become difficult to differentiate on MRI; this process has been described by Kostovic et al as the “resolution of the subplate”[24], which ultimately results in consolidation of these two layers to form the “mature” fetal cerebral white matter [25]. Independent of these changes, myelination begins at approximately 25 weeks of GA, with the earliest detectable histologic findings in the posterior limb of the internal capsules, posterior globus pallidus, and ventral lateral thalamus[26,27]. From there on, myelination progresses along white matter tracts in caudal-to-rostral, central-to-peripheral, and anterior-to-posterior direction[28,29]. It is well known that myelination results in increase in FA and decreased MD[30].

The non-linear GA- and tract-specific trends observed in our tractography analysis reflect the varying influence of these processes on the diffusivity characteristics of the fetal brain. The distinct GA-related increase in FA and decrease in MD that is seen in all tracts after 30 weeks of GA is consistent with the anatomic progression of myelination[11]. Even though some pre-myelination and myelination changes are known to occur prior to this age, the consolidation of this trend appears to coincide chronologically with the “resolution stage” of the fetal subplate and intermediate zone as well as more widespread and robust myelination on histology[3,27]. At GA less than 30 weeks, the microstructural changes of the transient fetal zones play a dominant role. For most tracts (forceps minor, ILF, IFOF, UF), there was a significant decrease in FA and increase in MD with GA in this time period. These changes correspond with the layer-specific diffusion and volumetric changes described above (see paragraph above). Specifically, the age-related

decrease in FA in the cortex and intermediate zone and the expansion of the subplate (with its low FA and high MD), contribute to these observations. Given that the long white matter bundles traverse these layers, the large effects of the layer-specific microstructural properties on whole-tract estimates is expected **(Supplementary Fig. 1)**.

Tractography of the CST deserves special mention. In fetuses < 27 weeks, the CST tracking terminates within the intermediate zone, without appreciable fiber tracking along the subplate or extension to the primary motor cortex. Review of the raw data, with lax deterministic tractography parameters (no exclusion ROIs), shows crossing fibers headed toward the lateral parietal and frontal regions. This is probably secondary to fiber tracking along the radial glial scaffolding that predominates in the second trimester; the former, in conjunction with the inherent limitation of the diffusion tensor model to resolve crossing fibers, results in the incomplete delineation of the tract [8] (**Supplementary Fig. 2**). The missing segment of the tract corresponds to the SP and CP voxels; given the large relative volume of the SP in this developmental stage and the dominant diffusion features of this layer, we believe that this contributes to the lack of significant change in FA or MD before 30 weeks of GA.

We also observed substantial within tract heterogeneity in microstructural development of the CST, forceps major, and IFOF. The presence of distinct developmental trajectories for segments within a single white matter tract suggests that tract averaged MD and FA are insufficient to capture the complex developmental changes of fetal brain development. The advantage of more precise spatial analyses has been documented postnatally. Colby et al., showed that within-tracts analysis outlined microstructural differences in children with fetal alcohol spectrum disorders that were not apparent on the tract-averaged analyses[31]. Our data, albeit limited to selected white matter tracts, are similar. For instance, most of the peripheral /telencephalic components of tracts (CST: superior segment; IFOF: rostral and caudal segments; forceps major: peripheral segments), showed an inflection point or nadir in FA at 29–32 weeks of GA. These findings were not apparent on tract-averaged analysis of the CST or forceps major as they were probably averaged with other components of the tracts. The central components of the tracts (CST: mid segment; IFOF: mid segment; forceps major: central segment) showed different trends. In all of these, the FA showed a continued linear increase with age, an effect that is likely dominated by density of axonal packing and myelination, as these segments do not traverse the telencephalic layers. The forceps major does show a peak around 30 weeks, that is likely driven by the other effects of axonal organization. Finally, the caudal segment of the CST shows the fastest rate of increase in FA of all CST segments at < 30 weeks of GA, which is consistent with the early myelination of the brainstem which precedes supratentorial myelination; subsequently, the rate of change decreases as myelination of these segment of the CST is largely complete by the mid third trimester. The set of ROIs chosen for this analysis are based solely on anatomy; however, future work will be focused on developing robust tools for along tract analysis that incorporate growth and change in geometry of individual white matter tracts. Improvement in these tools will improve our ability to correlate these findings with patterns of gene expression, early functional specialization, and selective vulnerability to injury.

This study has several limitations. Our analysis is based on a single-tensor model of the diffusion signal. This approach is sufficient to characterize tissue coherence along major white matter tracts; however, it imposes limitations related to crossing fibers which, as our data show, can impact the ability to delineate the anatomy of fetal white matter tracts and impact the reliability of the microstructural analysis. Future work utilizing other models of diffusion signal processing, including diffusion compartment imaging, are expected to improve our ability to resolve these structures[32]. Additionally, our analysis of within tract changes are based on anatomic parcellations of the white matter; although these convincingly demonstrate the heterogeneity of the white matter maturation, they do not perform direct spatial correspondence or enable group wise comparisons. Development of novel methods that allow for such analyses, analogous to those existing for post-natal pipelines[31], will significantly improve our ability to study brain maturation in utero.

Conclusion

Diffusion-atlas based tractography shows the white matter cytoarchitectonics drive diffusivity and anisotropy in the second and early third trimester and that myelination becomes a dominant factor in the mid to late third trimester. Our analysis also showed significant within-tract heterogeneity in development, highlighting the need to develop tools that permit robust along-tract analyses.

References

1. Andescavage, N. N. *et al.* Complex Trajectories of Brain Development in the Healthy Human Fetus. *Cereb Cortex.* **27**, 5274–5283 (2017).
2. Bystron, I., Blakemore, C. & Rakic, P. Development of the human cerebral cortex: Boulder Committee revisited. *Nat Rev Neurosci.* **9**, 110–122 (2008).
3. Brody, B. A., Kinney, H. C., Kloman, A. S. & Gilles, F. H. Sequence of central nervous system myelination in human infancy. I. An autopsy study of myelination. *J. Neuropathol. Exp. Neurol.* **46**, 283–301 (1987).
4. Vasung, L. *et al.* Ex vivo fetal brain MRI: Recent advances, challenges, and future directions. *NeuroImage.* **195**, 23–37 (2019).
5. Vasung, L. *et al.* Quantitative and Qualitative Analysis of Transient Fetal Compartments during Prenatal Human Brain Development. *Front Neuroanat.* **10**, 11 (2016).
6. Huang, H. & Vasung, L. Gaining insight of fetal brain development with diffusion MRI and histology. *Int J Dev Neurosci.* **32**, 11–22 (2014).
7. Song, J. W. *et al.* Asymmetry of White Matter Pathways in Developing Human Brains. *Cereb. Cortex.* **25**, 2883–2893 (2015).
8. Xu, G. *et al.* Radial Coherence of Diffusion Tractography in the Cerebral White Matter of the Human Fetus: Neuroanatomic Insights. *Cereb. Cortex.* **24**, 579–592 (2014).

9. Schneider, M. M. *et al.* Normative apparent diffusion coefficient values in the developing fetal brain. *AJNR Am J Neuroradiol.* **30**, 1799–1803 (2009).
10. Kasprian, G. *et al.* In utero tractography of fetal white matter development. *Neuroimage.* **43**, 213–224 (2008).
11. Jaimes, C. *et al.* In vivo characterization of emerging white matter microstructure in the fetal brain in the third trimester. *Human Brain Mapping* **n/a**,.
12. Yeh, F. C. *et al.* Population-averaged atlas of the macroscale human structural connectome and its network topology. *Neuroimage.* **178**, 57–68 (2018).
13. Yu, Q. *et al.* Structural Development of Human Fetal and Preterm Brain Cortical Plate Based on Population-Averaged Templates. *Cereb Cortex.* **26**, 4381–4391 (2016).
14. Khan, S. *et al.* Fetal brain growth portrayed by a spatiotemporal diffusion tensor MRI atlas computed from in utero images. *Neuroimage.* **185**, 593–608 (2019).
15. Kainz, B. *et al.* Fast Volume Reconstruction From Motion Corrupted Stacks of 2D Slices. *IEEE Trans. Med. Imaging.* **34**, 1901–1913 (2015).
16. Marami, B. *et al.* Motion-Robust Diffusion-Weighted Brain MRI Reconstruction Through Slice-Level Registration-Based Motion Tracking. *IEEE Trans Med Imaging.* **35**, 2258–2269 (2016).
17. Marami, B. *et al.* Temporal slice registration and robust diffusion-tensor reconstruction for improved fetal brain structural connectivity analysis. *Neuroimage.* **156**, 475–488 (2017).
18. Wang, R., Benner, T., Sorensen, A. G. & Wedeen, V. J. Diffusion Toolkit: A Software Package for Diffusion Imaging Data Processing and Tractography. in Proc. Intl. Soc. Mag. Reson. Med. vol. 15 3720(2007).
19. de Rodrigues, M. *et al.* K. A FreeSurfer-compliant consistent manual segmentation of infant brains spanning the 0â€“2 year age range.*Front. Hum. Neurosci.***9**, (2015).
20. Catani, M. & de Thiebaut, M. A diffusion tensor imaging tractography atlas for virtual in vivo dissections. *Cortex.* **44**, 1105–1132 (2008).
21. Yushkevich, P. A., Gao, Y., Gerig, G. & null & ITK-SNAP: An interactive tool for semi-automatic segmentation of multi-modality biomedical images. *Annu Int Conf IEEE Eng Med Biol Soc.* **2016**, 3342–3345 (2016).
22. McKinstry, R. C. *et al.* Radial organization of developing preterm human cerebral cortex revealed by non-invasive water diffusion anisotropy MRI. *Cereb Cortex.* **12**, 1237–1243 (2002).
23. Widjaja, E. *et al.* Alteration of human fetal subplate layer and intermediate zone during normal development on MR and diffusion tensor imaging. *AJNR Am J Neuroradiol.* **31**, 1091–1099 (2010).
24. Kostovic, I. & Rakic, P. Developmental history of the transient subplate zone in the visual and somatosensory cortex of the macaque monkey and human brain. *J Comp Neurol.* **297**, 441–470 (1990).
25. Vasung, L. *et al.* Quantitative In vivo MRI Assessment of Structural Asymmetries and Sexual Dimorphism of Transient Fetal Compartments in the Human Brain. *Cereb. Cortex.*

https://doi.org/10.1093/cercor/bhz200 (2019).

26. Jaimes, C. *et al.* Association of Isolated Congenital Heart Disease with Fetal Brain Maturation. AJNR Am J Neuroradiol ajnr;ajnr.A6635v1(2020) doi:10.3174/ajnr.A6635.
27. Kinney, H. C., Brody, B. A., Kloman, A. S. & Gilles, F. H. Sequence of central nervous system myelination in human infancy. II. Patterns of myelination in autopsied infants. *J. Neuropathol. Exp. Neurol.* **47**, 217–234 (1988).
28. Counsell, S. J. *et al.* MR imaging assessment of myelination in the very preterm brain. *AJNR Am J Neuroradiol.* **23**, 872–881 (2002).
29. Abe, S., Takagi, K., Yamamoto, T., Okuhata, Y. & Kato, T. Semiquantitative assessment of myelination using magnetic resonance imaging in normal fetal brains. *Prenat Diagn.* **24**, 352–357 (2004).
30. Neil, J. J. *et al.* Normal brain in human newborns: apparent diffusion coefficient and diffusion anisotropy measured by using diffusion tensor MR imaging. *Radiology.* **209**, 57–66 (1998).
31. Colby, J. B. *et al.* Along-tract statistics allow for enhanced tractography analysis. *NeuroImage.* **59**, 3227–3242 (2012).
32. Scherrer, B. *et al.* Characterizing brain tissue by assessment of the distribution of anisotropic microstructural environments in diffusion-compartment imaging (DIAMOND). *Magnetic Resonance in Medicine.* **76**, 963–977 (2016).

Tables

Table 1: Subjects of DTI atlas

Gestational Week	Number of Subjects	Sex (males)
23	8	5 *
24	9	6 *
25	8	5
26	11	4
27	11	4
28	9	7
29	11	8
30	10	7
31	10	9
32	9	7
33	9	6 *
34	7	4 *
35	5	5
36	5	4
37	5	4
38	5	4

DTI=Diffusion tensor imaging. *Indicates at least one subject with unknown sex at time of scan.

Table 2: Whole-tract analysis of rate of microstructure change.

Tract	FA / gestational week [95% CI]		MD / gestational week [95% CI]	
	All ages		≤30	>30
Forceps major	0.00302*** [0.00195 - 0.00408]		0.01532* [0.0039 - 0.02696]	-0.04260*** [(-0.05261) – (-0.03259)]
	≤30	>30	≤30	>30
Forceps minor	-0.00734** [(-0.01133) – (-0.00334)]	0.00102 [(-0.00241) - 0.00446]	0.03166*** [0.01875 - 0.04457]	-0.0168** [(-0.02793) – (-0.00573)]
	≤30	>30	≤30	>30
CST†	0.00038 [(-0.00108) - 0.001787]	0.00759*** [0.00635 - 0.00882]	0.01652** [0.00696 - 0.02609]	-0.03240*** [(-0.04062) - (-0.02417)]
	≤30	>30	≤30	>30
IFOF†	-0.00132** [(-0.00212) - (-0.00051)]	0.00347*** [0.00277 - 0.00416]	0.03027*** [0.02494 - 0.03561]	-0.03060*** [(-0.03518) - (-0.02601)]
	≤30	>30	≤30	>30
ILF†	-0.00456*** [(-0.00592) - (-0.00319)]	0.00268*** [0.00150 - 0.00385]	0.02946*** [0.02401 - 0.03491]	-0.03717*** [(-0.04186) – (-0.03248)]

	≤30	>30	≤30	>30
UF†	-0.00019 [(-.00128) - 0.00089]	0.00193*** [0.00010 - 0.00286]	0.014344* [0.00356 - 0.0251]	-0.01816*** [(-0.02744) - (-0.00888)]

FA Fractional anisotropy, MD Mean diffusivity, CST Corticospinal tract, IFOF Inferior fronto-occipital fasciculus, ILF Inferior longitudinal fasciculus, UF Uncinate fasciculus. * P < 0.050, ** P < 0.010, *** P < 0.001. †FA and MD of left and right tracts not significantly different (P > 0.050).

Table 3: Along-tract analysis of rate of microstructure change.

	Segment	FA / gestational week [95% CI]		MD / gestational week [95% CI]	
Forceps major		All ages		≤30	>30
	Anterior	0.00159 [(-0.0003855) – (0.0035669)]		0.01059 [(-0.00697) - 0.02816]	-0.03217*** [(-0.04729) – (-0.01706)]
		≤30	>30	≤30	>30
	Posterior	-0.00564*** [(-0.00719) – (-0.00409)]	-0.00009 [(-0.00143) – 0.00124]	0.02652** [0.01215 - 0.04089]	-0.04529*** [(-0.05765) – (-0.03292)]
CST		≤30	>30	All ages	
	Superior	-0.00927*** [(-0.01138) – (-0.00715)]	0.00744*** [0.00562 - 0.00926]	-0.02103** [(-0.03506) – (0.00699]	
		All ages		All ages	
	Middle	0.00691*** [0.00545 - 0.00838]		-0.01996* [(-0.03632) - (-0.00359)]	
		≤30	>30	All ages	
	Inferior	0.00493** [0.00148 - 0.00838]	0.00097 [(-0.00200) - 0.00394]	-0.01036 [(-0.03091) - (-0.01018)]	

IFOF		≤30	>30	≤30	>30
	Rostral	-0.00327*** [(-0.00456) – (-0.00197)]	-0.00025 [(-0.00136) - 0.00086]	0.04244*** [0.02541 - 0.05947]	-0.02102** [(-0.03567) - (-0.00637)]
		≤30	>30	≤30	>30
	Middle	0.000609 [(-0.00251) - 0.00373]	0.00562** [0.00294 - 0.00831]	0.02417* [0.00692 - 0.04142]	-0.02769*** [(-0.04253) – (-0.01285)]
		≤30	>30	≤30	>30
	Caudal	-0.00584*** [(-0.00809) – (-0.00359)]	0.00295** [0.00101 - 0.00489]	0.03453*** [0.02251 - 0.04655]	-0.03618*** [(-0.04651) – (-0.02584)]

FA Fractional anisotropy, MD Mean diffusivity, CST Corticospinal tract, IFOF Inferior fronto-occipital fasciculus. * P < 0.050, ** P < 0.010, *** P < 0.001.

Figures

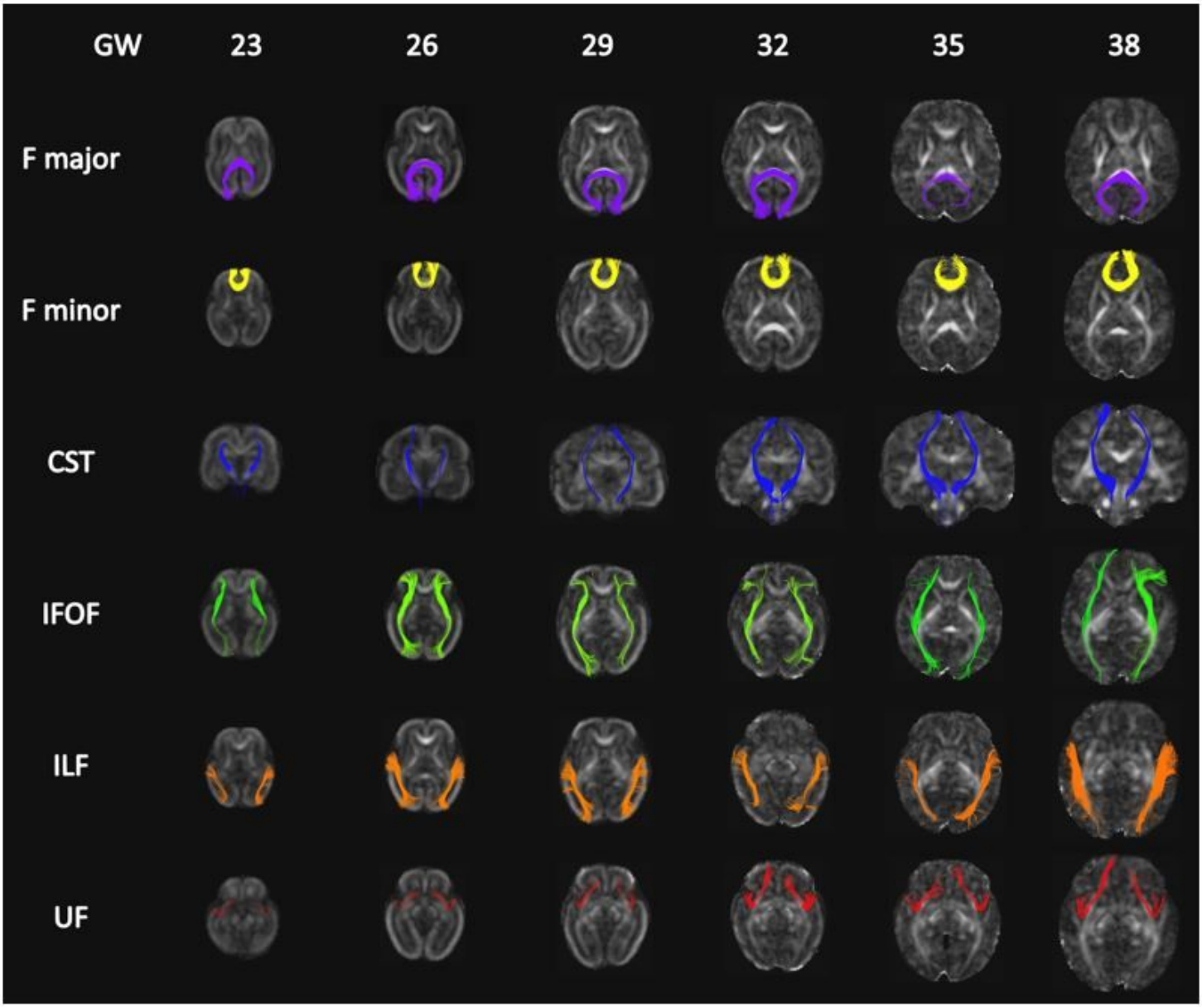

Figure 1

Longitudinal tractography of the fetal DTI templates Deterministic tractography on selected GA templates; tracts are superimposed on the corresponding FA map. The outlined tracts include forceps major (F major), forceps minor (F minor), corticospinal tract (CST), inferior fronto-occipital fasciculus (IFOF), inferior longitudinal fasciculus (ILF), and uncinate fasciculus (UF).

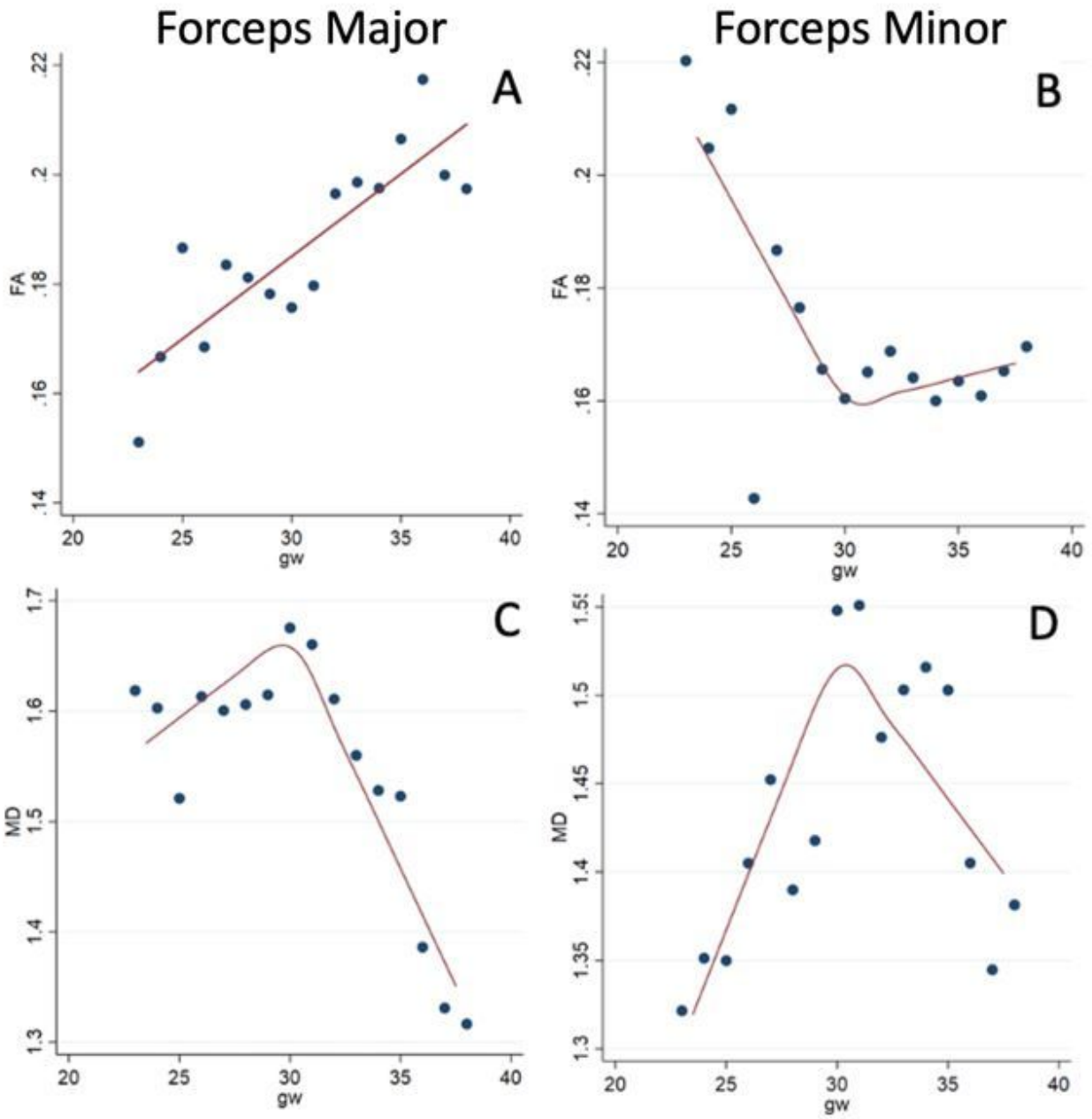

Figure 2

Whole-tract analysis of commissural tracts GA-related changes in FA and MD in the forceps major (A,C) and forceps minor (B, D). Linear spline regression lines is shown for A, and linear regression line with a prespecified regression knot at 30 gestational weeks is shown for B, C, and D. Rate of change and statistical significance are shown in Table 2.

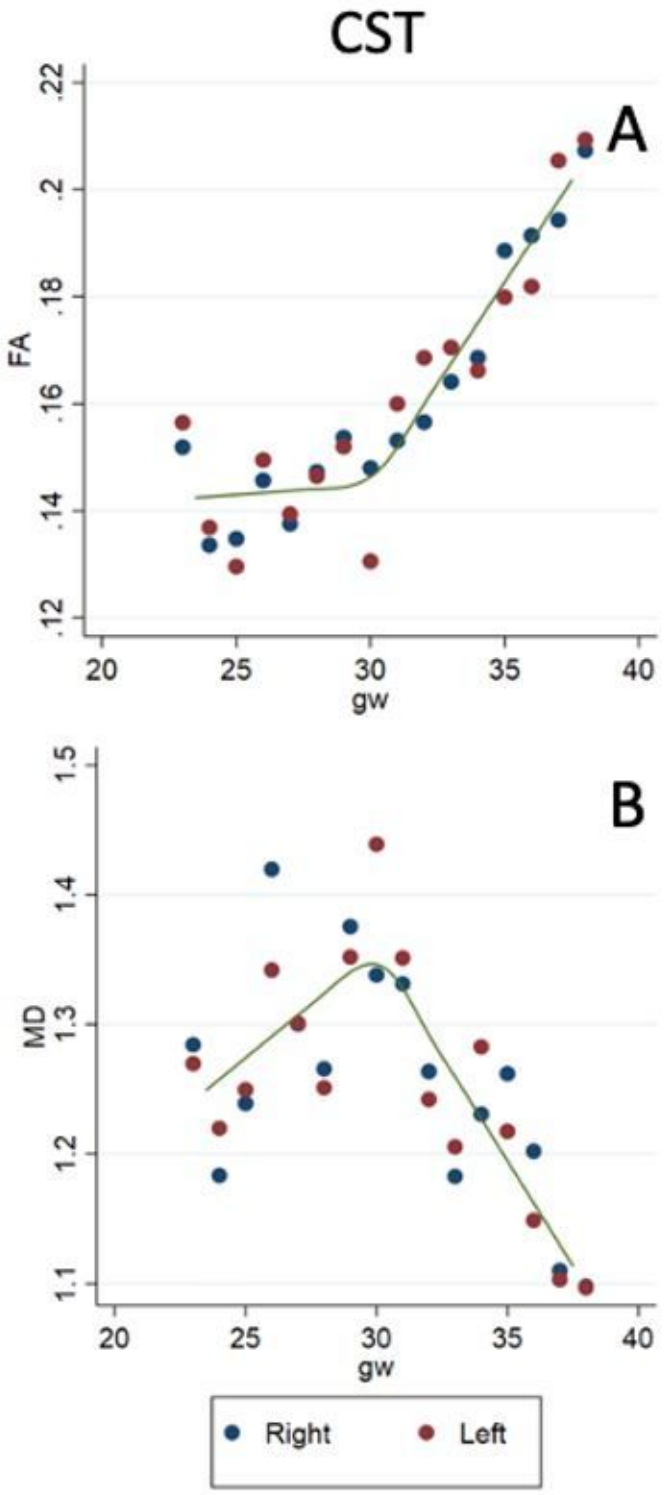

Figure 3

Whole-tract analysis of projection tracts GA-related changes in FA and MD in the CST. Linear spline regression lines are shown with prespecified regression knot at 30 gestational weeks, rate of change and significance is shown in Table 2. Laterality was included in the regression model, but was not statistically significant ($P > 0.05$).

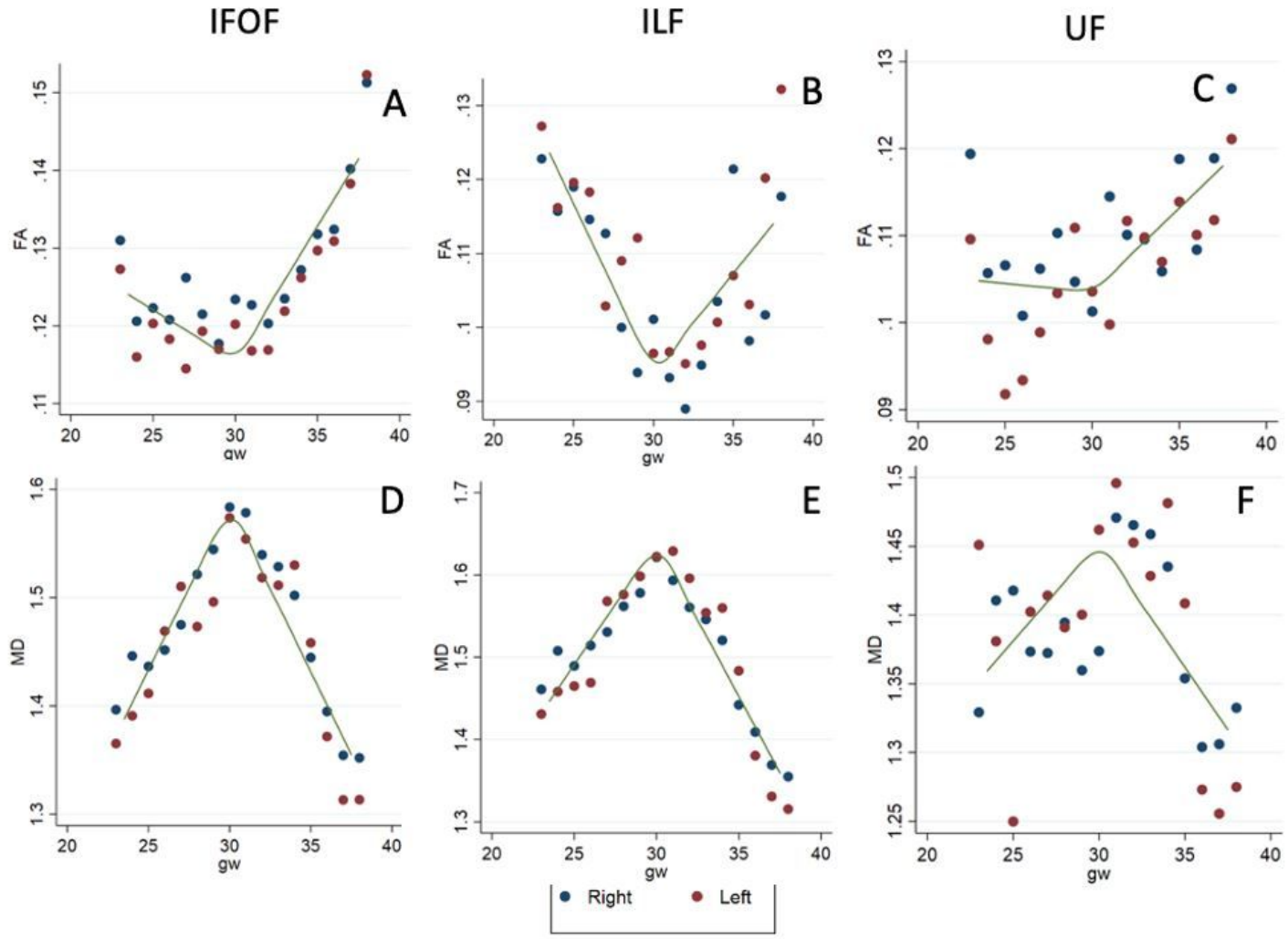

Figure 4

Whole-tract analysis of association tracts GA-related changes in FA and MD in the inferior fronto-occipital fasciculus (IFOF) (A,D), inferior longitudinal fasciculus (ILF) (B,E), and uncinate fasciculus (UF) (C, F). Linear regression line with a prespecified regression knot at 30 gestational weeks is shown. Rate of change and significance are shown in Table 2. Laterality was included in the regression model but was not statistically significant ($P > 0.05$) for any tract.

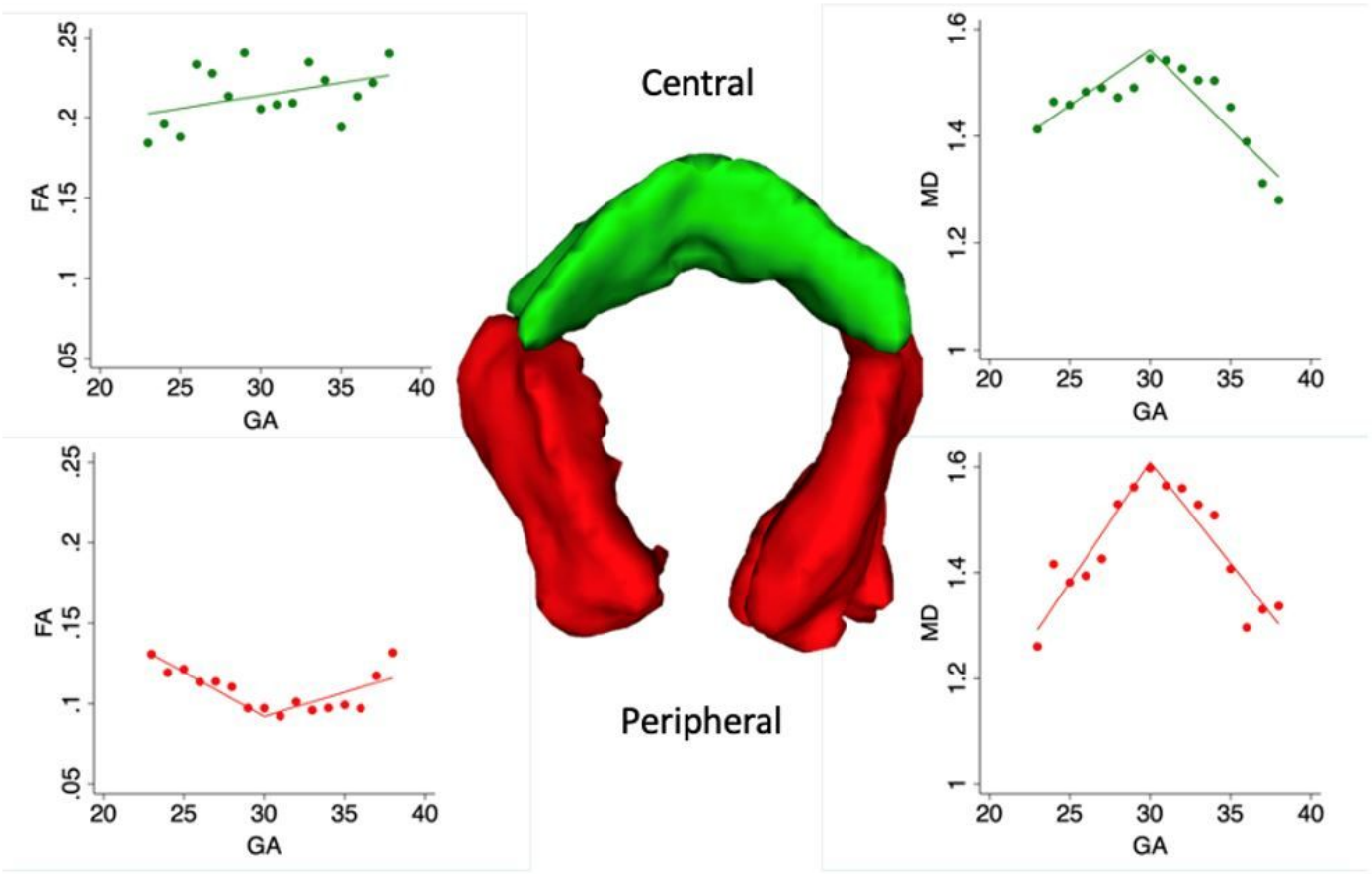

Figure 5

Within-tract analysis of forceps major Microstructural changes in the central (green) and peripheral (red) segments of the forceps major. The central segment shows gestational age (GA) -related increase in FA whereas the peripheral segment shows a decrease in FA. The MD of both segments shows a similar pattern, with a peak around 30 weeks of gestational age (GA). Rate of change and significance are shown in Table 3.

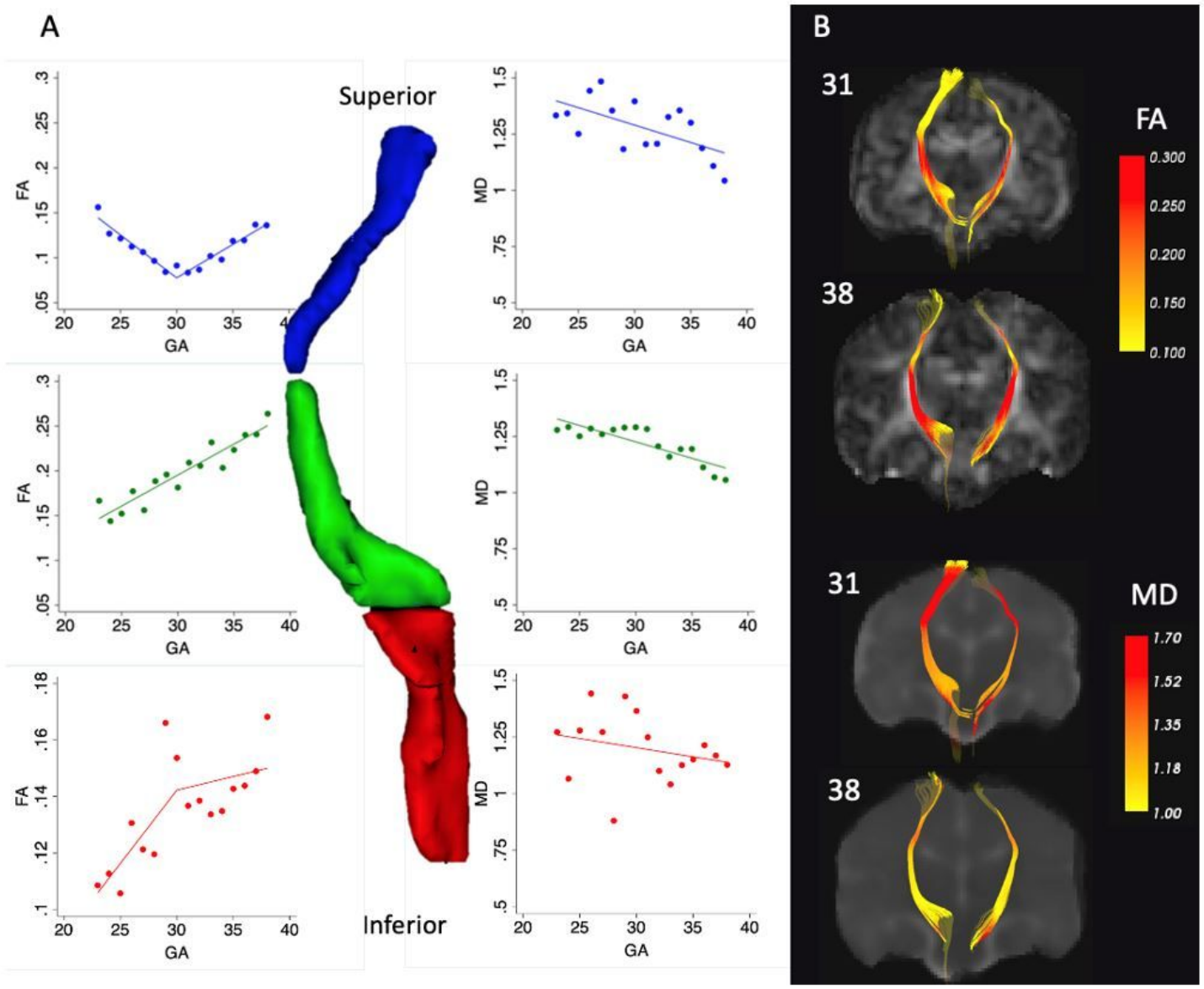

Figure 6

Within-tract analysis of CST Heterogeneity in development of the CST. (A) Microstructural changes in the superior (blue), mid (green), and inferior (red) segments of the CST. The superior segment shows nadir in FA at approximately 30 weeks of gestational age (GA). The mid segment shows linear GA-related increase in FA and decrease in MD. The inferior segment shows an increase in FA early in the second trimester with lower rate of change later in gestation. Rates of change and significance are shown in Table 3. (B) Heat maps of FA and MD at 31 and 38 weeks of GA show within tract heterogeneity in progression of microstructural changes.

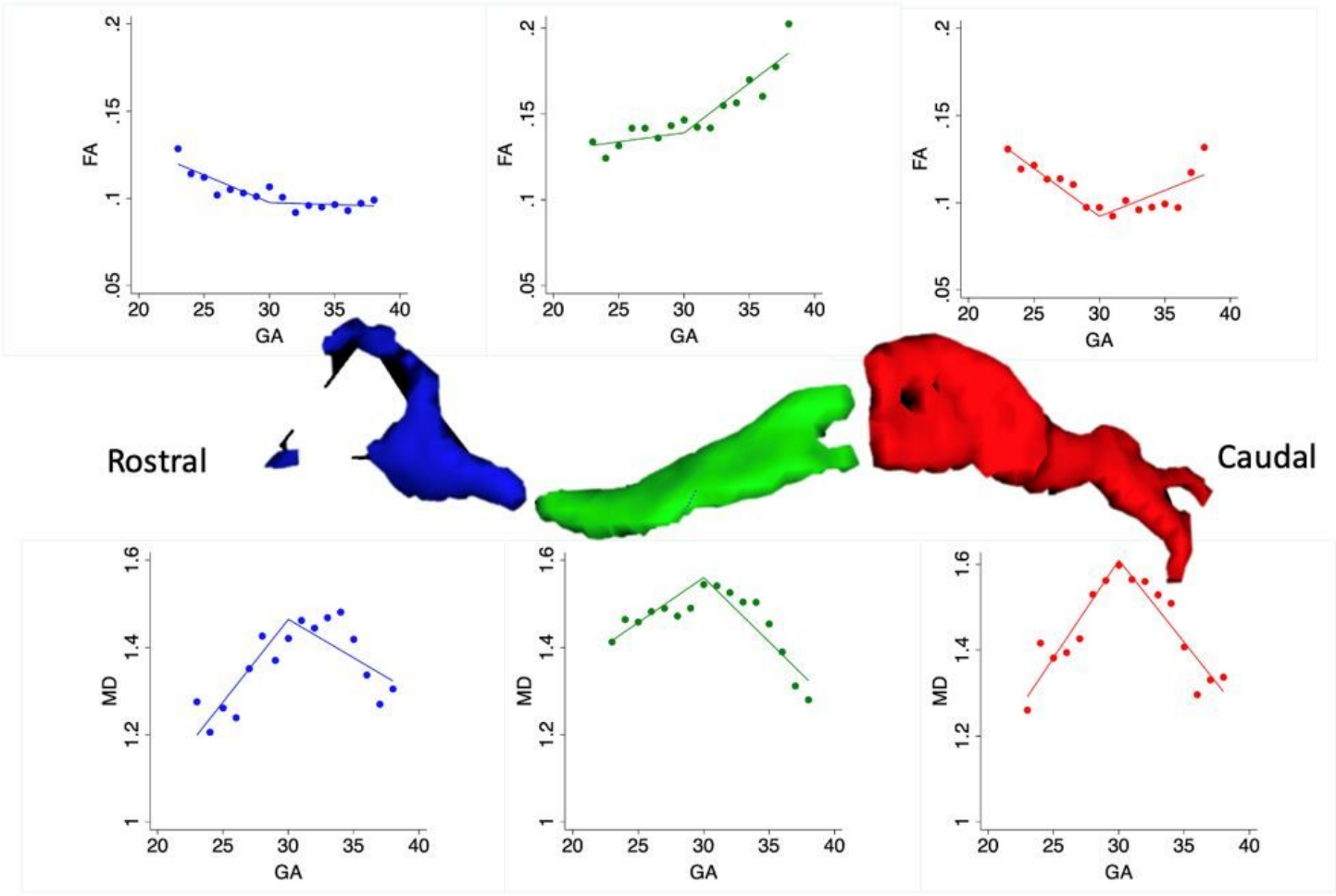

Figure 7

Within-tract analysis of IFOF Microstructural changes in the rostral (blue), mid (green), and caudal (red) segments of the IFOF. The rostral and caudal segments shows a decrease in FA at <30 weeks of GA probably as a result of expansion of the subplate. After > 30 weeks of GA, the caudal segment shows GA-related increase in FA that exceeds that of the rostral segment, representing the expected progression of myelination. The mid segment shows a continuous GA- related increase in FA as it is not influenced by changes in transient telencephalic zones. For all segments, the MD shows central peak, although the trajectories are slightly different. Rates of change and significance are shown in Table 3.

Supplementary Files

This is a list of supplementary files associated with this preprint. Click to download.

- SupplementaryFigures.docx